Morning Glucagon Disrupts Insulin Induced Hepatic Metabolic Memory and Subsequent Afternoon Glucose Metabolism in Canines

Hannah L. Waterman[1], Marta S. Smith[1], Ben Farmer[1], Kalisha Yankey[1], Karin J. Bosma[1], Richard M. O'Brien[1], Derek P. Claxton[1], Tristan Howard[1], Guillaume Kraft[1], Alan D. Cherrington[1], Dale S. Edgerton[1]

[1]Department of Molecular Physiology & Biophysics, Vanderbilt University School of Medicine

Corresponding author information:

Name: Hannah Waterman

Current Affiliation: Vanderbilt University School of Medicine

Phone: (360)-536-1498

Email: Hannah.L.Waterman@Vanderbilt.Edu

Running title: Hepatic Glucagon Memory Alters PM Glucose Metabolism

Conflict of Interest. A.D.C. has research contracts with Alnylam, Abvance, Fluidics, and Novo Nordisk, as well as grants from the NIH. A.D.C. is a consultant to Novo Nordisk, Paratus, Portal Insulin, and Fractyl. No other individuals have conflicts of interest relevant to this article.

Abstract

The Staub-Traugott effect describes the improved glycemic response observed after consuming a second identical meal. We previously showed that morning (AM) hyperinsulinemia primes the liver for enhanced afternoon (PM) meal-associated net hepatic glucose uptake (NHGU) and glycogen storage. However, depending on the meal composition, both insulin and glucagon may rise. Therefore, we investigated whether AM hyperglucagonemia alters the priming effect of AM hyperinsulinemia on subsequent hepatic glucose metabolism. Dogs underwent a 4h AM hyperinsulinemic-euglycemic clamp paired with either basal (AM INS, n=8) or elevated glucagon (AM INS+GCG, n=8). After a 1.5h rest, dogs underwent a 2.5h PM hyperinsulinemic-hyperglycemic clamp designed to mimic postprandial conditions. AM hyperglucagonemia reduced PM NHGU through additive shifts in both hepatic glucose uptake and production, leading to lower direct glycogen synthesis and less glycolytic flux. Mechanistically, hepatic glucokinase protein was reduced in the AM INS+GCG vs. AM INS group, suggesting diminished capacity for glucose phosphorylation and lower intracellular G6P, a central node regulating downstream hepatic glucose metabolism. Thus, morning hepatic glucagon exposure diminishes insulin's ability to prime the liver, limiting net hepatic glucose uptake during a later meal. These results underscore how antecedent hormonal signals govern subsequent postprandial hepatic glucose metabolism.

Introduction

The body's metabolic response to the first meal of the day has marked effects on glucose regulation during subsequent meals, resulting in improved postprandial glucose handling during the second meal (1-4). We have shown that this response, known as the Staub-Traugott effect or second meal phenomenon**,** is a result of enhanced hepatic glucose uptake (HGU) and hepatic glycogen storage in the afternoon**,** processes that are altered by morning insulin exposure (5). While insulin is now recognized as a central driver of this response (5, 6), the contributions of other hormonal and metabolic factors remain incompletely understood.

Hepatic glucose metabolism operates within a broader systemic network, where signaling feedback loops with other tissues, mediated by hormones, nutrient flux, and neural pathways, help maintain whole-body energy balance (7-9). One key factor that may influence the second meal phenomenon is glucagon, best known for its prominent role as a counter-regulatory hormone. Glucagon acutely opposes insulin action in the liver by stimulating hepatic glucose production (HGP) through glycogenolysis and gluconeogenesis, with an initial pronounced effect on the former (10, 11)**.** Because insulin and glucagon are typically co-secreted in response to mixed meals, their interaction is critical for shaping postprandial glucose metabolism throughout the day (12, 13). Previous studies have also demonstrated that elevated glucagon levels can acutely reduce HGU and blunt glycogen synthesis during a single meal, even when insulin levels are high (14, 15). Notably, in individuals with prediabetes or type 2 diabetes, the postprandial glucagon response to mixed- or high-protein meals is often exaggerated compared to normoglycemic individuals, contributing to impaired glucose

homeostasis and increased risk of disease progression (13, 16-19). Disruptions in systemic insulin or glucagon dynamics can therefore lead to widespread metabolic dysregulation. While glucagon's acute effects are well characterized, its morning effects on glucose handling later in the day have never been investigated**.** These complex inter-meal regulatory networks require mechanistic studies that examine how the liver integrates both hormonal and metabolic signals across consecutive meals (20, 21).

Metabolic memory, which describes the ability of tissues to retain lasting effects in response to prior metabolic or nutritional exposures, is emerging as an important concept relevant to glucose regulation. Rather than resetting fully after each meal or physiological state, cells can carry forward molecular and functional "imprints" from past stimuli that shape subsequent responses (22, 23). For example, adipose tissue retains obesity-induced epigenetic modifications even after weight loss, reflecting a durable record of prior metabolic stress (24, 25). Likewise, skeletal muscle demonstrates persistent adaptations following exercise training or metabolic insults, suggesting a form of functional memory that extends beyond the initiating event (26-29). These findings highlight that metabolic responses are not merely acute but are conditioned by prior exposures which alter tissue sensitivity and systemic nutrient handling throughout the day and over time. Despite these observations, metabolic memory in the liver has yet to be clearly defined. It is well known that many hepatic cellular processes, including those regulating glycogen storage and transcriptional changes, are transient and reversible, raising the question of what capacity the liver possesses to remember past hormonal or nutritional signals (30).

We therefore aimed to determine whether a morning rise in glucagon alters the insulin-driven priming of afternoon HGU and glycogen storage. We hypothesize that morning hyperglucagonemia attenuates insulin's effects on afternoon hepatic glucose metabolism, potentially reducing the benefits of insulin priming from breakfast. By directly assessing these effects, we aim to clarify the interaction between insulin and glucagon across meals and determine how hormonal fluctuations shape hepatic glucose handling over time. This knowledge is important not only for understanding the mechanisms underlying the second meal effect but also for informing therapeutic strategies to be used in diabetes management, including dual-hormone insulin and glucagon pump systems or co-agonists designed to optimize glycemic control by leveraging the complementary actions of insulin and glucagon (31).

Research Design and Methods

Sex as a biological variable

Both male and female adult mongrel dogs were included in this study (16 males, 13 females). Animals were allocated such that each experimental group was balanced as closely as possible to a 1:1 male-to-female ratio. For the subset of dogs used for hepatic tissue collection at the 330-min time point, equal numbers of males and females were included. While sex differences were not the primary focus of this study, exploratory analyses did not reveal any significant sex-specific effects on hepatic glucose metabolism. Thus, the findings are expected to be relevant to both sexes, although the sample size limits definitive sex difference conclusions.

Animal care and surgical procedures

Dogs were used as the model because they allow optimal protocol design and precise assessment of hepatic metabolism in vivo. Their size enables catheterization and repeated sampling from both the portal and hepatic veins over many hours, an approach that is too invasive in humans and not feasible in rodents. This allows detailed flux analysis under controlled conditions *in vivo*. In addition, canine metabolism closely resembles that of humans, and their genomes share a high degree of similarity and conserved function, further supporting translational relevance (32-34). The study included a total of 29 adult mongrel dogs. 16 dogs (n=8 for each group: AM INS and AM INS+GCG) underwent the full experimental protocol, including a 4h AM hyperinsulinemic-euglycemic clamp, a 1.5h rest period, and a 2.5h afternoon hyperinsulinemic-hyperglycemic (HIHG) clamp (average weight 25.2 ± 0.8 kg). Tissues from 13 additional dogs were used exclusively for hepatic protein and molecular analyses and were not used for flux measurements. 5 dogs, which did not undergo any clamps, served as basal hepatic tissue controls, while 4 dogs from each of the AM INS and AM INS+GCG groups underwent only the AM clamp and rest period.

The animals were sourced from a USDA-licensed vendor and housed in accordance with the American Association for the Accreditation of Laboratory Animal Care guidelines. Two weeks prior to each experiment, a laparotomy was performed under general anesthesia to place blood flow probes around the hepatic artery and hepatic portal vein. Catheters for blood sampling were inserted into the hepatic vein, hepatic portal vein, and femoral artery, and infusion catheters were positioned in the splenic and jejunal veins (which supply the hepatic portal vein) and inferior vena cava.

The terminal ends of these catheters were secured subcutaneously until the study day. The dogs were maintained on a once-daily controlled diet consisting of chow and meat, providing 46% carbohydrate, 34% protein, 14.5% fat, and 5.5% fiber and fasted for 18h before the experiment. Health status was assessed based on meal intake (>75% of their last meal), leukocyte count (<18,000/mm^3), and hematocrit (>34%). Blood sampling was limited to ≤20% of total blood volume.

Experimental Design

The 8-hour experimental protocol included two clamping periods designed to mimic pancreatic hormone conditions at times corresponding to breakfast and lunch meals, denoted as the AM clamp (0-240 min) and the PM clamp (330-480 min), respectively **(Fig. 1)**. Blood was collected every 15–30 min from the femoral artery, hepatic portal vein, and hepatic veins for the measurement of hormone and substrate levels. Arterial plasma glucose was monitored every 5 min, and exogenous glucose infusion into a peripheral vein was adjusted as needed to ensure precise glucose control.

Morning (AM) Clamp Period (0-240 min)

We previously demonstrated that a physiological morning increase in insulin, rather than glucose, drives the hepatic metabolic memory that enhances afternoon HGU (5). Consequently, a hyperinsulinemic-euglycemic clamp was performed in the morning. At the start of the clamp, somatostatin (Bachem, Torrance, CA) was infused into the inferior vena cava (0.8 µg/kg/min) to suppress endogenous pancreatic insulin and

glucagon secretion. To replicate the physiologic insulin secretion pattern previously observed during a morning duodenal glucose infusion (5), insulin (Novolin R; Novo Nordisk, Basværd, Denmark) was infused intraportally at 2.1 mU/kg/min from 0-30 min, 2.4 mU/kg/min from 30-60 min, and 1.5 mU/kg/min from 60-240 min. Two experimental groups were studied. One group (AM INS) received a basal intraportal glucagon infusion (GlucaGen, Boehringer Ingelheim, Ridgefield, CT) at 0.57 ng/kg/min for 0-240 min, while the other group (AM INS + GCG) received an elevated, physiologic infusion of glucagon designed to maintain a consistent insulin-to-glucagon molar ratio over the AM clamp period, with infusion rates of 2.28 ng/kg/min from 0-30 min, 2.60 ng/kg/min from 30-60 min, and 1.63 ng/kg/min from 60–240 min. These two conditions were designed to replicate the hormonal milieu seen following the ingestion of a carbohydrate or mixed meal in the morning. Glucose was clamped at a euglycemic level (~100 mg/dL plasma glucose). To allow HGU and direct glycogen synthesis to be determined during the afternoon period, a peripheral infusion of [3-^{3}H]-glucose (Revvitty, Waltham, MA) was initiated at 180 min in both groups, with a priming dose of 38 µCi, followed by a continuous infusion at 0.38 µCi/min. At the conclusion of the AM clamp (240 min), all infusions, except for the tracer, were discontinued.

Non-clamp Period (240 – 330 min)

To evaluate glucose kinetics before initiating the PM clamp, blood samples were collected from the femoral artery, portal vein, and hepatic vein catheters at 300, 315, and 330 min (Fig. 1). To examine the liver's molecular profile at the start of the PM phase, a subset of dogs (*n=4*/group) were anesthetized with pentobarbital at 330 min,

after which hepatic tissue was rapidly harvested, immediately flash-frozen in liquid nitrogen to preserve cellular conditions, and stored at -80°C. Afterwards, the dogs were euthanized with pentobarbital.

Afternoon (PM) Clamp Period (330 – 480 min)

Both the AM INS and AM INS+GCG groups (n=8/group) underwent an identical 2.5h HIHG clamp during the afternoon phase **(Fig. 1).** Somatostatin was infused into a peripheral leg vein, while basal glucagon and fourfold basal insulin (1.2 mU/kg/min) were administered intraportally. To activate the portal glucose feeding signal, glucose was infused directly into the hepatic portal vein (4 mg/kg/min) (35). In addition, both groups received a primed, continuous glucose infusion into a peripheral vein to quickly bring glucose levels up to hyperglycemia (~200 mg/dL plasma glucose), where they were maintained for the entirety of the PM clamp. These conditions were designed to replicate, at steady-state, the metabolic environment seen following the ingestion of a carbohydrate-rich meal in the afternoon (36). After the final blood sample was obtained at 480 min, the dogs were anesthetized, and hepatic tissue was excised and preserved as described above. Following tissue collection, the dogs were euthanized.

Analyses

Biochemical and Molecular Methods

Whole blood samples were utilized to assess hormone and substrate flux across the liver using arteriovenous balance techniques (37). During the study, plasma glucose levels were measured in quadruplicate using an Analox GM9 glucose analyzer. Insulin

(#PI-12K, MilliporeSigma, Burlington, MA), glucagon (#GL-32K, MilliporeSigma), and cortisol (VUMC Analytical Services Core in-house primary antibody with I^{125} cortisol from MP Biomedicals, Santa Ana, CA) were quantified via radioimmunoassay (37). Glucagon values were background corrected to account for non-specific binding. This correction ensured that reported glucagon levels accurately reflected true circulating concentrations, strengthening the reliability of our hormonal flux analyses. Key metabolic intermediates, including lactate, glycerol, alanine, and non-esterified fatty acids (NEFAs), were measured using enzymatic spectrophotometric assays (37). Plasma samples were deproteinized using the Somogyi method and quantified via liquid scintillation counting to determine the specific activity of [3-^{3}H]-glucose in each sample (38, 39). Terminal hepatic glycogen was quantitatively assessed using the Keppler and Decker amyloglucosidase method (40).

Molecular analyses were performed on hepatic tissue collected at the beginning and at the end of the PM clamp, including qPCR analysis, western blotting, and enzymatic activity assays using radioisotope and colorimetric detection methods (37). Gene expression levels were normalized to GAPDH, while protein levels were standardized against total protein normalized to Ponceau S stain, as appropriate. Assays were optimized for canine-specific targets using validated antibodies and primers (41). Microsomal membranes were isolated from frozen liver, and glucose-6-phosphatase activity was measured *in vitro* using standard spectrophotometric methods (42). Detailed protocols for all methodologies, including reagents, primer sequences, antibody information, sample preparation, and calculations, are provided in the supplemental materials.

Calculations

Net hepatic glucose balance (NHGB) was determined using arterio-venous difference calculations, expressed as NHGB = $[HGL_{out}]$ - $[HGL_{in}]$. In this equation, HGL_{out} represents the glucose output from the liver and was computed as $[HGL_{out}] = [BF_h \times G_h]$, while HGL_{in} denotes the glucose entering the liver, calculated as $[HGL_{in}] = [(BF_a \times G_a) + (BF_p \times G_p)]$. Here, G represents blood glucose concentration, BF indicates measured blood flow, and A, P, and H correspond to the hepatic artery, hepatic portal vein, and hepatic vein, respectively. When HGU surpasses glucose production, NHGB is negative, indicating net glucose uptake (NHGU). This methodology was extended to assess net hepatic balance for various substrates and hormones across the liver. Hepatic fractional glucose extraction was determined by dividing NHGB by HGL_{in}. Unidirectional HGU was computed as the product of HGL_{in} and the fractional extraction of [3-^{3}H]-glucose. Non-HGU, attributed primarily to skeletal muscle glucose uptake, was derived by subtracting HGU from the glucose infusion rate (GIR) and correcting for glucose mass fluctuations over time. Direct glycogen synthesis, which quantifies glycogen formed directly from glucose taken up by the liver, was estimated by dividing the total radiolabeled glycogen stored in hepatic tissue by the specific activity of the glucose precursor pool. The radiolabeled glycogen measurement reflected total disintegrations per min (dpm) of labeled glucose incorporated into glycogen during the PM clamp, while the precursor pool's specific activity was determined as the ratio of labeled to unlabeled glucose (dpm/mg) in the inflowing blood, weighted by the relative contributions of the hepatic artery and portal vein. Hepatic sinusoidal plasma insulin and

glucagon concentrations were derived based on the relative contributions of the hepatic artery and portal vein flow to the liver, following established methodology (6). Total gluconeogenic flux was defined as the rate at which gluconeogenic precursors (alanine, glycerol, and lactate if it is taken up by the liver) were converted into glucose-6-phosphate (G6P), the central hepatic intermediate that can be dephosphorylated and released as glucose or directed toward glycogen synthesis. Alanine was doubled to account for net hepatic uptake of all amino acids, as alanine accounts for approximately 50% of gluconeogenic amino acid precursor uptake (41, 43). Fluxes from amino acids and glycerol were expressed in 3-carbon glucose equivalents and divided by 2 to account for the incorporation of two 3-carbon units into one 6-carbon G6P molecule. Glycolytic flux was estimated as the sum of net hepatic output of lactate and pyruvate (expressed in glucose equivalents) plus hepatic glucose oxidation. Pyruvate flux was approximated as 10% of lactate flux, reflecting the typical plasma pyruvate-to-lactate ratio under steady-state conditions (44). Hepatic glucose oxidation was assumed to be 0.2 mg/kg/min, consistent with previous clamp studies showing its stability and minimal contribution to overall hepatic glucose flux (45, 46). Net hepatic gluconeogenic/glycolytic flux (NHGNG) was calculated as NHGNG = glycolytic flux – gluconeogenic flux, such that positive values indicate net glycolysis, and negative values indicate net gluconeogenesis. Net glycogen flux (NHGLY) was then determined to reflect net glycogen synthesis/breakdown, with positive values representing glycogenesis and negative values representing glycogenolysis. Therefore, NHGLY = NHGU – NHGNG. Collectively, these approaches provide robust and reliable estimates of hepatic substrate and hormone fluxes (33).

Statistics

Data are expressed as mean ± SEM. A two-way repeated-measures ANOVA was conducted to evaluate differences between groups and changes over time in flux analyses, followed by Tukey's post hoc test for multiple comparisons. An unpaired two-tailed t-test was applied to analyze respective areas under the curve, while molecular analyses were assessed using a one-way ANOVA with Tukey's post hoc test. Normality of all datasets was confirmed using the Shapiro-Wilk test, and all data were found to follow a normal distribution. Statistical analyses were performed using GraphPad Prism software. Exact P values are reported where available; otherwise, significance is indicated by threshold values (e.g., $P < 0.05$, $P < 0.01$, $P < 0.001$, $P < 0.0001$). A significance threshold of $P < 0.05$ was applied.

Study approval

All procedures were approved by the Vanderbilt Institutional Animal Care and Use Committee. All experiments adhered to institutional and national guidelines for the care and use of laboratory animals.

Data availability

Values for all data points in graphs are reported in the Supporting Data Values file. Additionally, these data and supplemental materials are publicly available: doi.org/10.6084/m9.figshare.29988931. All other data generated and analyzed during the current study are available from the corresponding author upon reasonable request.

Results

AM Clamp Glucose and Hormone Data

During the AM clamp, euglycemia was successfully maintained in both groups **(Fig. 2A)**. Plasma insulin increased in a similar pattern across arterial, portal vein, and calculated hepatic sinusoidal sites in both the AM INS and the AM INS+GCG groups (**Fig. 2B-D Table 1).** Arterial plasma glucagon remained basal in the AM INS group (AM mean of 23 ± 1 pg/mL) but doubled in the AM INS+GCG group (AM mean of 49 ± 2 pg/mL; **Fig. 2E, Table 1).** Similar patterns were observed in portal vein and hepatic sinusoidal glucagon levels **(Fig. 2F, G, Table 1).** In the AM INS+GCG group, glucagon peaked at 60 min (arterial 71 ± 3 pg/mL; hepatic sinusoidal 116 ± 6 pg/mL) before gradually declining yet remained elevated relative to basal levels for the remainder of the clamp. Despite higher glucagon levels in the AM INS+GCG group, the glucose infusion rate required to maintain euglycemia was comparable between groups (mean of 9.5 ± 0.5 mg/kg/min in AM INS vs. 9.3 ± 1.3 mg/kg/min in AM INS + GCG, **Fig. 2H**). Net hepatic glucose balance switched from output to uptake in both groups, with no significant difference between the two groups **(Fig. 2I).**

After the 1.5h rest period, hormone and substrate levels had returned toward baseline, and all dogs were in a glucose-producing state. This reflects normalization of glucose homeostasis following the AM intervention and is evident across the 300 - 330 min period preceding the onset of the PM clamp.

PM Clamp Glucose and Hormone Data

The PM clamp was designed to mimic a postprandial hormonal and substrate milieu by maintaining hyperglycemia through peripheral (leg vein) glucose infusion, while concurrent portal vein glucose infusion established a physiologic meal-associated arterial-to-portal vein glucose gradient of ~20-25 mg/dL **(Fig. 3A-D).** Insulin levels were markedly elevated in both the arterial circulation and hepatic sinusoids (**Fig. 3E, F)**, whereas glucagon levels remained basal throughout the PM clamp **(Fig. 3G, H).** Thus, matching hormonal and glycemic conditions existed in both the AM INS and AM INS+GCG groups during the PM clamp.

The glucose infusion rate required to maintain hyperglycemia was similar in both groups during the PM clamp **(Fig. 4A, B).** Mean non-HGU was 7.6 ± 0.9 mg/kg/min in the AM INS group and 9.4 ± 1.3 mg/kg/min in the AM INS+GCG group, with no significant difference between the two groups **(Fig. 4C, D).** NHGU in the PM was 41% lower in the AM INS+GCG group (PM mean of 6.1 ± 0.6 vs. 3.6 ± 0.4 mg/kg/min in the AM INS vs. AM INS+GCG groups, respectively, $P < 0.0027$ **Fig. 4E, F).** This reduction occurred in conjunction with a non-significant difference in unidirectional HGU in the PM (mean of 5.7 ± 0.5 mg/kg/min vs. 5.0 ± 0.3 mg/kg/min in the AM INS vs. AM INS+GCG group**,** respectively; **Fig. 4G, H).** In contrast, HGP was fully inhibited in the AM INS group but averaged 1.4 ± 0.4 mg/kg/min in the AM INS+GCG group during the PM clamp. Although the HGP flux showed only a trend toward significance ($P = 0.06$, **Fig. 4I**), the ΔAUC was significantly higher in the AM INS+GCG group compared to AM INS **(Fig. 4J).** Consistent with this, net glycolytic flux was significantly lower in the AM INS+GCG group ($P < 0.024$; **Fig. 4K)**, and net glycogenic flux was also reduced by 41% ($P < 0.004$; **Fig. 4L)**. Together, these data demonstrate that prior morning hepatic

glucagon exposure reduced the ability of morning insulin to enhance hepatic glucose uptake and storage in the PM.

During the PM clamp, arterial plasma non-esterified fatty acid (NEFA) and glycerol levels, as well as hepatic uptake of both substrates, were similarly suppressed in the AM INS and AM INS+GCG groups, reflecting effective insulin-mediated inhibition of hepatic fatty acid handling under PM HIHG conditions **(Fig. 5A-D).** Circulating alanine levels and hepatic alanine balance remained stable throughout the PM clamp, with no differences between groups **(Fig. 5E, F)**. In contrast, arterial lactate concentrations and net hepatic lactate output were significantly lower in the AM INS+GCG group compared with the AM INS group (**Fig. 5G, H)**. These results indicate that prior morning glucagon exposure selectively diminished hepatic glucose flux during the PM clamp, while leaving lipid and amino acid handling largely unaffected.

Terminal Liver Biopsies

Terminal liver biopsies were first obtained at 330 min, following completion of the AM clamp and rest period but prior to initiation of the PM clamp **(Fig. 6A).** The 330 min time point was chosen to provide a baseline assessment of hepatic mRNA, protein, and metabolite levels prior to the PM clamp. Flux measurements diverge between groups immediately upon initiation of the PM clamp, indicating that hepatic molecular changes had already occurred by that time. At 330 min, no differences in Akt phosphorylation were observed among groups **(Fig. 6B).** Glucokinase (*GCK*) mRNA was significantly increased in the AM INS group compared with basal, whereas this induction was absent in AM INS+GCG **(Fig. 6C).** Consistent with transcript levels, GCK protein expression

was elevated only in AM INS **(Fig. 6D).** Total glucose-6-phosphatase (G6Pase) activity in intact and disrupted microsomes, measured using G6P as a substrate, was not different between the AM INS and AM INS+GCG groups at this time point **(Fig. 6E).** G6Pase activity in disrupted microsomes, measured using M6P as a substrate, also showed no difference. Phosphorylation of glycogen synthase (GS) did not differ between groups, either **(Fig. 6F).** Furthermore, phosphorylation and activity of glycogen phosphorylase (GP) were not significantly different between groups **(Fig. 6G, H).**

The second set of biopsies was collected at 480 min, at the conclusion of the PM clamp **(Fig. 7A).** Akt phosphorylation was significantly increased in AM INS and AM INS+GCG compared with Basal **(Fig. 7B).** *GCK* mRNA expression was induced in both groups compared to baseline **(Fig. 7C).** GCK protein remained significantly elevated only in AM INS, while levels in AM INS+GCG were not different from Basal **(Fig. 7D).** Total glucose-6-phosphatase activity and activity in intact microsomes remained similar between the AM INS and AM INS+GCG groups **(Fig. 7E).** GS phosphorylation was comparably reduced in both insulin groups **(Fig. 7F),** accompanied by increased GS activity **(Fig. 7G).** GP phosphorylation was reduced in both insulin groups compared with basal **(Fig. 7H),** while GP activity was not significantly different between any of the groups **(Fig. 7I).** Additionally, mean direct glycogen synthesis during the PM clamp (360-480 min) was significantly reduced in the AM INS+GCG group compared to the AM INS group (1.8 ± 0.2 vs. 3.2 ± 0.7 mg/kg/min, respectively, $P < 0.015$; **Fig. 7J).** In summary, AM insulin primed the liver by increasing *GCK* mRNA and protein prior to the PM clamp, whereas concurrent AM glucagon blocked GCK transcription and translation. Although downstream regulation of glycogen synthase and phosphorylase

were similar and *GCK* mRNA levels were comparable at the end of the PM clamp, only the AM INS group maintained elevated GCK protein, partially explaining the reduction observed in NHGU, glycolysis, and lactate release in the AM INS+GCG group. Supporting molecular data are shown in Supplemental Figures 1 and 2.

Summary of Hepatic Fluxes

Figure 8 summarizes integrated hepatic glucose fluxes during the PM clamp. In the AM INS group, NHGU was relatively large, reflecting sustained hepatic glucose retention following morning insulin exposure. This was entirely due to HGU, as HGP remained fully suppressed. Incoming glucose was phosphorylated to G6P, which was either stored as glycogen or metabolized through glycolysis and released as lactate or oxidized. In contrast, when glucagon accompanied insulin in the morning, PM NHGU was lower, driven by a combination of a non-significant decrease in HGU and sustained HGP relative to the AM INS group. Additionally, less G6P was partitioned into glycolytic and glycogenic pathways. Together, these combined effects produced substantially lower hepatic glucose retention. These findings demonstrate that antecedent glucagon exposure induces metabolic memory, blunting insulin-mediated stimulation of NHGU and glycogen synthesis.

Discussion

The regulation of hepatic glucose metabolism is central to maintaining systemic glucose homeostasis. Breakfast plays a pivotal role in postprandial glycemic control and glycogen storage, influencing the metabolic response to subsequent meals in both

healthy individuals and those with diabetes (2-4, 47, 48). Skipping breakfast has been associated with an increased risk of developing type 2 diabetes, suggesting that disruptions in morning nutrient and hormone signaling can have persistent effects on glucose metabolism and overall metabolic health (49, 50). Although the precise contribution of glucagon to metabolic dysregulation remains incompletely understood, postprandial hyperglucagonemia is consistently observed in obesity and type 2 diabetes, potentially impairing glucose homeostasis by limiting insulin-mediated glucose uptake and sustaining hepatic glucose production (13, 51-53). Since glucagon opposes insulin's anabolic actions by promoting glycogenolysis and glucose output, understanding its impact on postprandial metabolism is particularly important given that the insulin-to-glucagon ratio governs hepatic metabolic balance (54). These considerations prompted us to investigate whether elevated morning glucagon impairs the insulin-mediated enhancement of afternoon glucose disposal.

Our findings are the first to demonstrate that antecedent morning glucagon exposure reprograms hepatic glucose metabolism thereby impacting NHGU and glycogen deposition later in the day. This highlights the sensitivity of the liver to changes in insulin and glucagon occurring even hours beforehand and underscores their importance to subsequent intracellular substrate partitioning and enzymatic regulation. These findings indicate that, like insulin, prior glucagon exposure establishes hepatic metabolic memory. Following morning glucagon exposure, afternoon carbon flux shifts away from storage and toward re-release, thereby attenuating insulin's contribution to the second-meal effect.

Several mechanistic factors likely contributed to the reduced PM NHGU observed in the AM INS+GCG group. Central among these is glucokinase, a key rate-controlling enzyme in hepatic glucose metabolism, the activity of which correlates with HGU (48). The morning rise in glucagon in the AM INS+GCG group appears to have blunted insulin's effect on hepatic *GCK* mRNA and protein later in the day. We hypothesize this effect reduced glucose phosphorylation, subsequently diminishing the hepatic G6P pool in the AM INS+GCG group and limiting substrate availability for glycogen synthesis and glycolysis (55). Downstream enzymes, including GS and GP, showed no differences in dephosphorylation or intrinsic activity; however, a reduced G6P pool in the AM INS+GCG group would theoretically diminish allosteric activation of GS and relieve inhibition of GP, effects that are not fully captured by our protein abundance measurements or standard activity assays (56). Additionally, HGP remained significant in the AM INS+GCG group during the PM HIHG clamp, while it was effectively suppressed in the AM INS group. Since G6Pase activity was similar between groups, the enzymatic machinery to convert G6P back to glucose was clearly sufficient for ongoing HGP in the AM INS+GCG group and therefore not rate controlling in the AM INS group. Instead, suppression of HGP in the AM INS group was likely due to the pull of G6P into the glycogenic and glycolytic pathways mediated by GCK induced increases in G6P (57). In contrast, the sustained HGP in the AM INS+GCG group was likely due to increased glycogenolysis, which would result from reduced GCK generated G6P (58). This flux model is consistent with the observed difference in net flux between G6P and glycogen between groups, as gluconeogenic fluxes were minimal and comparable. Importantly, flux measurements provide a more accurate reflection of hepatic glucose

handling than static molecular readouts (59). Together, these results indicate that antecedent glucagon reprograms hepatic glucose flux by targeting GCK, the primary regulatory constraint, limiting substrate availability for glycogen synthesis and glycolysis.

To understand the molecular mechanisms underlying our findings, we measured hepatic *GCK* mRNA and protein levels over the course of the study (basal, prior to, and at the end of the PM period). As expected, based on the well-established effects of insulin on *GCK* transcription, 5.5h after the start of the insulin prime hyperinsulinemia had increased *GCK* mRNA and protein in the AM INS group. Glucagon, however, blocked the transcriptional and translational effects of insulin during the morning. A precedent for this was previously demonstrated *in vitro*. In cultured rat hepatocytes, glucagon rapidly repressed insulin-stimulated *GCK* transcription via a cAMP-dependent pathway under supramaximal insulin conditions, reducing mRNA accumulation within 30-45 minutes (60). Furthermore, in hepatocytes in which *GCK* transcription had already been induced by prolonged insulin exposure, glucagon (or a cAMP analog) also accelerated degradation of existing *GCK* mRNA, with an apparent half-life of ~45 minutes (60).

During the PM clamp, hyperinsulinemia in the AM INS group maintained the equilibrium of mRNA transcription and degradation that was established during the morning period, such that *GCK* mRNA remained similar at the 330 min and 480 min time points. As a result, GCK protein levels also remained elevated. This suggests that the insulin-dependent homeostatic setpoint for *GCK* mRNA and protein levels was similar during the two periods. In contrast, at the end of the PM clamp *GCK* mRNA levels, but not protein, were elevated in the AM INS + GCG group. This was to be

expected, however, since we have previously shown that it typically requires two to four hours to show a measurable increase in GCK protein following mRNA induction by insulin (61). Thus, the 2.5h hyperinsulinemic PM period was long enough to increase *GCK* mRNA but not protein. Notably, although total hepatic GCK protein levels at the end of the PM clamp were similar between the basal and AM INS+GCG groups, it is important to consider subcellular localization. Glucokinase regulatory protein dynamically modulates GCK by sequestering it in the nucleus during low-glucose conditions and releasing it into the cytoplasm when glucose is abundant (55, 62, 63). Therefore, it is plausible that a larger fraction of GCK in the AM INS+GCG group resides in the cytosolic, active compartment, which could help explain why HGU remains elevated in the AM INS+GCG group despite similar total GCK protein levels to basal tissue. This highlights that total protein measurements alone may not fully capture the functional state of GCK *in vivo*. Although this mechanism remains speculative in vivo, it highlights that the molecular processes by which morning glucagon disrupts insulin-driven GCK accumulation and hepatic glucose flux are not fully understood and warrant further investigation. The use of complementary models that allow more detailed mechanistic exploration beyond what is feasible in the canine model will be important to clarify these processes (62).

Several points should be considered when interpreting these findings. First, tissue analyses at fixed time points may have missed transient flux regulators or dynamic enzyme activity, since steady-state protein abundance and in vitro enzyme assays cannot fully capture allosteric regulation or compartmentalization of metabolite pools (6). Future studies investigating subcellular compartmentalization, glycogen-

associated microdomains, and allosteric regulation of glycogen enzymes will be useful for a complete understanding of hepatic glucose retention in the context of the second meal phenomenon (20, 64). Clamp studies provide the advantage of tightly regulating hormone and substrate concentrations, allowing precise assessment of their effects on hepatic glucose metabolism. However, it is important to note that our experimental design, which involved prolonged glucagon elevation for 4 hours alongside concurrent hyperinsulinemia during the morning clamp, does not fully replicate the dynamic hormonal environment elicited by a typical mixed or high-protein meal, in which glucagon typically rises and falls within one to two hours depending on meal composition (65, 66). Consequently, while our findings clarify the role of sustained glucagon exposure in reprogramming hepatic glucose flux, they may not directly predict the magnitude or timing of the second-meal effect under physiological dietary conditions. The canine model, with its unique vascular access to the liver and the gut, offers the flexibility to study both clamp and meal conditions. In this study, clamps were used to isolate the direct effects of morning insulin and glucagon, allowing individual contributions to be evaluated before adding the complexity of mixed meals in future studies. Additionally, while hyperglucagonemia was modeled to maintain a physiologic insulin-to-glucagon molar ratio, this approach may not fully replicate the timing, magnitude, or dynamics of glucagon release during mixed or high-protein meals. Despite significant progress, many aspects of glucagon physiology remain poorly understood, particularly its interactions with other hormones and its diverse roles in hepatic and systemic metabolic pathways (67, 68). Continued research is important to

unravel these complexities and guide development of effective therapies targeting glucagon signaling.

In conclusion, morning glucagon exposure induced hepatic metabolic memory, reprogramming glucose metabolism and influencing glucose homeostasis later in the day. Specifically, morning glucagon reduced PM NHGU, limited glycogen synthesis, and blunted the suppression of PM HGP during an afternoon HIHG clamp. Mechanistically, this effect reflected constraints on insulin-stimulated glucose phosphorylation by GCK, probably leading to substrate-driven limitations on hepatic glycogen storage and glycolysis. These findings identified glucagon as a key regulator of hepatic glucose partitioning and highlighted the critical role of early meal-associated insulin-glucagon interactions in shaping the liver's response to subsequent meals.

Acknowledgments

Author Contributions. H.W., D.S.E., and A.D.C. contributed to the design of the experiments. H.W. directed all experiments and collected data. H.W., B.F., K.Y., and T.H. participated in experimental execution. B.F. and K.Y. were responsible for surgical preparation and oversight of animal care. H.W. and M.S.S. performed biochemical and tissue analyses. K.J.B., R.M.O., and D.P.C. designed and carried out the G6Pase activity assays. H.W., D.S.E., and A.D.C. interpreted the experimental results. H.W. prepared figures and drafted the manuscript, and H.W., D.S.E., G.K., and A.D.C. edited and revised it. All authors approved the final version of the manuscript.

Guarantor Statement. A.D.C. is the guarantor of this work and, as such, has full access to all the data in the study and takes responsibility for the integrity of the data and the accuracy of the data analysis.

Funding. This work was supported by National Institutes of Health (NIH) grant R01DK131082 (to A.D.C), R01DK132259 (to R.O'B) and R01GM149686 (to D.P.C). H.W. was supported by NIH grant F31DK142297 and by the Vanderbilt University Training Program in Molecular Endocrinology NIH grant T32DK007563. Hormone analysis was completed by Vanderbilt's Hormone Assay and Analytical Services Core, supported by NIH grants DK020593 and DK059637. Vanderbilt's Large Animal Core provided surgical expertise, supported by the NIH Grant DK020593.

Prior Presentation. This work was presented at the American Diabetes Association 2024 meeting. The abstract can be viewed at doi.org/10.2337/db24-1565-P.

References

1. Chowdhury EA, Richardson JD, Tsintzas K, Thompson D, and Betts JA. Carbohydrate-rich breakfast attenuates glycaemic, insulinaemic and ghrelin response to ad libitum lunch relative to morning fasting in lean adults. *Br J Nutr.* 2015;114(1):98-107.
2. Abraira C, Buchanan B, and Hodges L. Modification of glycogen deposition by priming glucose loads: the second-meal phenomenon. *Am J Clin Nutr.* 1987;45(5):952-7.

3. Jovanovic A, Gerrard J, and Taylor R. The second-meal phenomenon in type 2 diabetes. *Diabetes Care.* 2009;32(7):1199-201.

4. Jovanovic A, Leverton E, Solanky B, Ravikumar B, Snaar JE, Morris PG, et al. The second-meal phenomenon is associated with enhanced muscle glycogen storage in humans. *Clin Sci (Lond).* 2009;117(3):119-27.

5. Moore MC, Smith MS, Farmer B, Coate KC, Kraft G, Shiota M, et al. Morning Hyperinsulinemia Primes the Liver for Glucose Uptake and Glycogen Storage Later in the Day. *Diabetes.* 2018;67(7):1237-45.

6. Waterman HL, Moore MC, Smith MS, Farmer B, Yankey K, Scott M, et al. Improved Afternoon Hepatic Glucose Disposal and Storage Requires Morning Engagement of Hepatic Insulin Receptors. *Diabetes.* 2024.

7. Rojas JM, and Schwartz MW. Control of hepatic glucose metabolism by islet and brain. *Diabetes Obes Metab.* 2014;16 Suppl 1(0 1):33-40.

8. Poggiogalle E, Jamshed H, and Peterson CM. Circadian regulation of glucose, lipid, and energy metabolism in humans. *Metabolism.* 2018;84:11-27.

9. Lin EE, Scott-Solomon E, and Kuruvilla R. Peripheral Innervation in the Regulation of Glucose Homeostasis. *Trends Neurosci.* 2021;44(3):189-202.

10. Ramnanan CJ, Edgerton DS, Kraft G, and Cherrington AD. Physiologic action of glucagon on liver glucose metabolism. *Diabetes Obes Metab.* 2011;13 Suppl 1(Suppl 1):118-25.

11. Jiang G, and Zhang BB. Glucagon and regulation of glucose metabolism. *Am J Physiol Endocrinol Metab.* 2003;284(4):E671-8.

12. Hatting M, Tavares CDJ, Sharabi K, Rines AK, and Puigserver P. Insulin regulation of gluconeogenesis. *Ann N Y Acad Sci.* 2018;1411(1):21-35.

13. Alsalim W, Tura A, Pacini G, Omar B, Bizzotto R, Mari A, et al. Mixed meal ingestion diminishes glucose excursion in comparison with glucose ingestion via several adaptive mechanisms in people with and without type 2 diabetes. *Diabetes Obes Metab.* 2016;18(1):24-33.

14. Holste LC, Connolly CC, Moore MC, Neal DW, and Cherrington AD. Physiological changes in circulating glucagon alter hepatic glucose disposition during portal glucose delivery. *Am J Physiol.* 1997;273(3 Pt 1):E488-96.

15. Rivera N, Ramnanan CJ, An Z, Farmer T, Smith M, Farmer B, et al. Insulin-induced hypoglycemia increases hepatic sensitivity to glucagon in dogs. *J Clin Invest.* 2010;120(12):4425-35.

16. Park YM, Heden TD, Liu Y, Nyhoff LM, Thyfault JP, Leidy HJ, et al. A high-protein breakfast induces greater insulin and glucose-dependent insulinotropic peptide responses to a subsequent lunch meal in individuals with type 2 diabetes. *J Nutr.* 2015;145(3):452-8.

17. Lund A, Bagger JI, Christensen M, Knop FK, and Vilsbøll T. Glucagon and type 2 diabetes: the return of the alpha cell. *Curr Diab Rep.* 2014;14(12):555.

18. Fonseca VA. Defining and characterizing the progression of type 2 diabetes. *Diabetes Care.* 2009;32 Suppl 2(Suppl 2):S151-6.

19. Hædersdal S, Lund A, Knop FK, and Vilsbøll T. The Role of Glucagon in the Pathophysiology and Treatment of Type 2 Diabetes. *Mayo Clin Proc.* 2018;93(2):217-39.

20. Han HS, Kang G, Kim JS, Choi BH, and Koo SH. Regulation of glucose metabolism from a liver-centric perspective. *Exp Mol Med.* 2016;48(3):e218.

21. Hunter AL, and Bechtold DA. The metabolic significance of peripheral tissue clocks. *Communications Biology.* 2025;8(1):497.

22. Dong H, Sun Y, Nie L, Cui A, Zhao P, Leung WK, et al. Metabolic memory: mechanisms and diseases. *Signal Transduction and Targeted Therapy.* 2024;9(1):38.

23. Chen Z, and Natarajan R. Epigenetic modifications in metabolic memory: What are the memories, and can we erase them? *Am J Physiol Cell Physiol.* 2022;323(2):C570-c82.

24. Hinte LC, Castellano-Castillo D, Ghosh A, Melrose K, Gasser E, Noé F, et al. Adipose tissue retains an epigenetic memory of obesity after weight loss. *Nature.* 2024;636(8042):457-65.

25. Cottam MA, Caslin HL, Winn NC, and Hasty AH. Multiomics reveals persistence of obesity-associated immune cell phenotypes in adipose tissue during weight loss and weight regain in mice. *Nat Commun.* 2022;13(1):2950.

26. Sharples AP, and Turner DC. Skeletal muscle memory. *Am J Physiol Cell Physiol.* 2023;324(6):C1274-c94.

27. Pilotto AM, Turner DC, Mazzolari R, Crea E, Brocca L, Pellegrino MA, et al. Human skeletal muscle possesses an epigenetic memory of high-intensity interval training. *Am J Physiol Cell Physiol.* 2025;328(1):C258-c72.

28. Gattu AK, Tanzer M, Yaron-Barir TM, Johnson JL, Jayavelu AK, Pan H, et al. Cell-intrinsic insulin signaling defects in human iPS cell-derived hepatocytes in type 2 diabetes. *J Clin Invest.* 2025;135(8).

29. Batista TM, Jayavelu AK, Wewer Albrechtsen NJ, Iovino S, Lebastchi J, Pan H, et al. A Cell-Autonomous Signature of Dysregulated Protein Phosphorylation Underlies Muscle Insulin Resistance in Type 2 Diabetes. *Cell Metab.* 2020;32(5):844-59.e5.

30. Rui L. Energy metabolism in the liver. *Compr Physiol.* 2014;4(1):177-97.

31. Infante M, Baidal DA, Rickels MR, Fabbri A, Skyler JS, Alejandro R, et al. Dual-hormone artificial pancreas for management of type 1 diabetes: Recent progress and future directions. *Artif Organs.* 2021;45(9):968-86.

32. Domínguez-Oliva A, Hernández-Ávalos I, Martínez-Burnes J, Olmos-Hernández A, Verduzco-Mendoza A, and Mota-Rojas D. The Importance of Animal Models in Biomedical Research: Current Insights and Applications. *Animals (Basel).* 2023;13(7).

33. Cherrington AD. Banting Lecture 1997. Control of glucose uptake and release by the liver in vivo. *Diabetes.* 1999;48(5):1198-214.

34. Shearin AL, and Ostrander EA. Leading the way: canine models of genomics and disease. *Dis Model Mech.* 2010;3(1-2):27-34.

35. Myers SR, McGuinness OP, Neal DW, and Cherrington AD. Intraportal glucose delivery alters the relationship between net hepatic glucose uptake and the insulin concentration. *J Clin Invest.* 1991;87(3):930-9.

36. Moore MC, Coate KC, Winnick JJ, An Z, and Cherrington AD. Regulation of hepatic glucose uptake and storage in vivo. *Adv Nutr.* 2012;3(3):286-94.

37. Waterman HL, Moore MC, Smith M, Farmer B, Scott M, Edgerton DS, et al. Duration of Morning Hyperinsulinemia is Key to the Enhancement of Hepatic Glucose Uptake and Glycogen Storage Later in the Day. *bioRxiv.* 2024:2024.05.10.593551.

38. Sindelar DK, Balcom JH, Chu CA, Neal DW, and Cherrington AD. A Comparison of the Effects of Selective Increases in Peripheral or Portal insulin on Hepatic Glucose Production in the Conscious Dog. *Diabetes.* 1996;45(11):1594-604.

39. Nelson N. A PHOTOMETRIC ADAPTATION OF THE SOMOGYI METHOD FOR THE DETERMINATION OF GLUCOSE. *Journal of Biological Chemistry.* 1944;153(2):375-80.

40. Keppler D, and Decker K. Academic Press, New York and London; 1974.

41. Edgerton DS, Cardin S, Emshwiller M, Neal D, Chandramouli V, Schumann WC, et al. Small Increases in Insulin Inhibit Hepatic Glucose Production Solely Caused by an Effect on Glycogen Metabolism. *Diabetes.* 2001;50(8):1872-82.

42. Hawes EM, Rahim M, Haratipour Z, Orun AR, O'Rourke ML, Oeser JK, et al. Biochemical and metabolic characterization of a G6PC2 inhibitor. *Biochimie.* 2024;222:109-22.

43. Shah AM, and Wondisford FE. Tracking the carbons supplying gluconeogenesis. *J Biol Chem.* 2020;295(42):14419-29.

44. Redant S, Hussein H, Mugisha A, Attou R, De Bels D, Honore PM, et al. Differentiating Hyperlactatemia Type A From Type B: How Does the Lactate/pyruvate Ratio Help? *J Transl Int Med.* 2019;7(2):43-5.

45. Moore MC, Satake S, Lautz M, Soleimanpour SA, Neal DW, Smith M, et al. Nonesterified fatty acids and hepatic glucose metabolism in the conscious dog. *Diabetes.* 2004;53(1):32-40.

46. Satake S, Moore MC, Igawa K, Converse M, Farmer B, Neal DW, et al. Direct and indirect effects of insulin on glucose uptake and storage by the liver. *Diabetes.* 2002;51(6):1663-71.

47. Maki KC, Phillips-Eakley AK, and Smith KN. The Effects of Breakfast Consumption and Composition on Metabolic Wellness with a Focus on Carbohydrate Metabolism. *Adv Nutr.* 2016;7(3):613s-21s.

48. Petersen MC, Vatner DF, and Shulman GI. Regulation of hepatic glucose metabolism in health and disease. *Nat Rev Endocrinol.* 2017;13(10):572-87.

49. Ma X, Chen Q, Pu Y, Guo M, Jiang Z, Huang W, et al. Skipping breakfast is associated with overweight and obesity: A systematic review and meta-analysis. *Obes Res Clin Pract.* 2020;14(1):1-8.

50. Bi H, Gan Y, Yang C, Chen Y, Tong X, and Lu Z. Breakfast skipping and the risk of type 2 diabetes: a meta-analysis of observational studies. *Public Health Nutr.* 2015;18(16):3013-9.

51. Honka H, Koffert J, Kauhanen S, Kudomi N, Hurme S, Mari A, et al. Liver blood dynamics after bariatric surgery: the effects of mixed-meal test and incretin infusions. *Endocr Connect.* 2018;7(7):888-96.

52. Wikarek T, Kocełak P, Owczarek AJ, Chudek J, and Olszanecka-Glinianowicz M. Effect of dietary macronutrients on postprandial glucagon and insulin release in obese and normal-weight women. *Int J Endocrinol.* 2020;2020:4603682.

53. Herman GA, Bergman A, Stevens C, Kotey P, Yi B, Zhao P, et al. Effect of single oral doses of sitagliptin, a dipeptidyl peptidase-4 inhibitor, on incretin and plasma glucose levels after an oral glucose tolerance test in patients with type 2 diabetes. *J Clin Endocrinol Metab.* 2006;91(11):4612-9.

54. Kalra S, and Gupta Y. The Insulin:Glucagon Ratio and the Choice of Glucose-Lowering Drugs. *Diabetes Ther.* 2016;7(1):1-9.

55. Agius L. Hormonal and Metabolite Regulation of Hepatic Glucokinase. *Annu Rev Nutr.* 2016;36:389-415.

56. Velho G, Petersen KF, Perseghin G, Hwang JH, Rothman DL, Pueyo ME, et al. Impaired hepatic glycogen synthesis in glucokinase-deficient (MODY-2) subjects. *J Clin Invest.* 1996;98(8):1755-61.

57. Abu Aqel Y, Alnesf A, Aigha, II, Islam Z, Kolatkar PR, Teo A, et al. Glucokinase (GCK) in diabetes: from molecular mechanisms to disease pathogenesis. *Cell Mol Biol Lett.* 2024;29(1):120.

58. Aiston S, Andersen B, and Agius L. Glucose 6-phosphate regulates hepatic glycogenolysis through inactivation of phosphorylase. *Diabetes.* 2003;52(6):1333-9.

59. Bar-Peled L, and Kory N. Principles and functions of metabolic compartmentalization. *Nat Metab.* 2022;4(10):1232-44.

60. Iynedjian PB, Jotterand D, Nouspikel T, Asfari M, and Pilot PR. Transcriptional induction of glucokinase gene by insulin in cultured liver cells and its repression by the glucagon-cAMP system. *J Biol Chem.* 1989;264(36):21824-9.

61. Ramnanan CJ, Edgerton DS, Rivera N, Irimia-Dominguez J, Farmer B, Neal DW, et al. Molecular characterization of insulin-mediated suppression of hepatic glucose production in vivo. *Diabetes.* 2010;59(6):1302-11.

62. Cullen KS, Al-Oanzi ZH, O'Harte FP, Agius L, and Arden C. Glucagon induces translocation of glucokinase from the cytoplasm to the nucleus of hepatocytes by transfer between 6-phosphofructo 2-kinase/fructose 2,6-bisphosphatase-2 and the glucokinase regulatory protein. *Biochim Biophys Acta.* 2014;1843(6):1123-34.

63. Agius L. Glucokinase and molecular aspects of liver glycogen metabolism. *Biochemical Journal.* 2008;414(1):1-18.

64. Habashy A, Acree C, Kim K-Y, Zahraei A, Dufresne M, Phan S, et al. Spatial patterns of hepatocyte glucose flux revealed by stable isotope tracing and multi-scale microscopy. *Nature Communications.* 2025;16(1):5850.

65. Ichikawa R, Takano K, Fujimoto K, Kobayashi M, Kitamura T, Shichiri M, et al. Robust increase in glucagon secretion after oral protein intake, but not after glucose or lipid intake in Japanese people without diabetes. *J Diabetes Investig.* 2023;14(10):1172-4.

66. Kabadi UM. Dose-kinetics of pancreatic α- and β-cell responses to a protein meal in normal subjects. *Metabolism - Clinical and Experimental.* 1991;40(3):236-40.

67. Capozzi ME, D'Alessio DA, and Campbell JE. The past, present, and future physiology and pharmacology of glucagon. *Cell Metab.* 2022;34(11):1654-74.

68. Finan B, Capozzi ME, and Campbell JE. Repositioning Glucagon Action in the Physiology and Pharmacology of Diabetes. *Diabetes.* 2020;69(4):532-41.

Table 1 - Plasma hormone concentrations measured during the AM clamp

	Group	
AM Clamp Parameter	**AM INS (*n=8*)**	**AM INS+GCG (*n=8*)**
Arterial Plasma Insulin (µU/mL)	50 ± 4	51 ± 4
Hepatic Sinusoidal Plasma Insulin (µU/mL)	151 ± 6	170 ± 15
Arterial Plasma Glucagon (pg/mL)	23 ± 1	49 ± 2****
Hepatic Sinusoidal Plasma Glucagon (pg/mL)	34 ± 3	81 ± 3****

Data are presented as mean ± SEM. Insulin samples were analyzed every 30 min, and glucagon samples were analyzed every hour during the experimental protocol. Each value represents the mean of all samples collected within each clamping period (n = 8/group). ****P < 0.0001.

Figure Legends

1. **Figure 1. Experimental protocol.** Canines underwent a 4h euglycemic clamp in the morning (AM; 0-240 min). Somatostatin (SST) was infused to suppress endogenous secretion of glucagon (GCG) and insulin (INS). Insulin was replaced in a pattern mimicking levels previously observed during a duodenal glucose

infusion. One group received basal glucagon (AM INS), while the other received hyperglucagonemia (AM INS+GCG) in a pattern maintaining an equal molar ratio between insulin and glucagon throughout the AM clamp. A tracer infusion was initiated near the end of the AM clamp (180 min) to allow equilibration before the start of the PM clamp. Following the AM clamp, there was a 1.5h rest period (240-330 min) during which all infusions were halted. At the end of this period, a subset of dogs (n = 4/group) was euthanized for hepatic tissue collection and molecular analysis. The remaining dogs (n = 8/group) underwent a 2.5h PM HIHG clamp with portal glucose delivery (330-480 min), after which hepatic tissue was collected. Additional details are provided in the Methods section.

2. **Figure 2. Morning (AM) clamp glucose and hormone flux data.** (A) Arterial plasma glucose, (B) arterial plasma insulin, (C) portal vein plasma insulin, (D) hepatic sinusoidal plasma insulin, (E) arterial plasma glucagon, (F) portal vein plasma glucagon, (G) hepatic sinusoidal plasma glucagon, (H) glucose infusion rate, and (I) net hepatic glucose balance (negative values indicate uptake, positive values indicate output) are shown for the AM INS and AM INS+GCG groups (n = 8/group) throughout the AM clamp. Data are expressed as mean ± SEM. ***P < 0.001, ****P < 0.0001 between groups; ns = non-significant.

3. **Figure 3. Afternoon (PM) clamp glucose and hormone flux data.** A vertical line at 330 min indicates the end of the rest period and the onset of the PM clamp. (A) Arterial plasma glucose, (B) portal vein plasma glucose, (C) arterial–portal glucose difference, (D) hepatic glucose load, (E) arterial plasma insulin, (F) hepatic sinusoidal plasma insulin, (G) arterial plasma glucagon, and (H) hepatic

sinusoidal plasma glucagon are shown throughout the 2.5h hyperinsulinemic-hyperglycemic PM clamp in both the AM INS and AM INS+GCG groups (n = 8/group). No significant differences were observed between groups for any measured parameter. Data are expressed as mean ± SEM; ns = non-significant.

4. **Figure 4. Glucose uptake and storage during the PM hyperinsulinemic-hyperglycemic clamp.** A vertical line at 330 min indicates the end of the rest period and the onset of the PM clamp. (A) Glucose infusion rate (GIR), (B) GIR ΔAUC, (C) non-hepatic glucose uptake (NHGU), (D) NHGU ΔAUC, (E) net hepatic glucose uptake (NHGU; values >0 indicate uptake, <0 indicate output), (F) NHGU ΔAUC, (G) unidirectional hepatic glucose uptake determined using tritiated glucose, (H) HGU AUC, (I) hepatic glucose production (HGP; determined from the difference between NHGU and HGU), (J) HGP AUC, (K) net gluconeogenic/glycolytic flux (values >0 indicate net glycolysis, <0 indicate net gluconeogenesis), and (L) net glycogen flux (values >0 indicate net glycogenesis, <0 indicate net glycogenolysis) are shown over time for the AM INS and AM INS+GCG groups (n = 8/group). Data are expressed as mean ± SEM. *P < 0.05, **P < 0.01 between groups; ns = non-significant.

5. **Figure 5: PM clamp fatty acid and metabolite flux data.** A vertical line at 330 min separates the resting period from the onset of the PM clamp. (A) Arterial plasma non-esterified fatty acids (NEFA), (B) net hepatic NEFA uptake, (C) arterial blood glycerol, (D) net hepatic glycerol uptake, (E) arterial blood alanine, (F) net hepatic alanine uptake, (G) arterial blood lactate, and (H) net hepatic lactate uptake are shown throughout the PM HIHG clamp for the AM INS and AM

INS+GCG groups (n = 8/group). Data are expressed as mean ± SEM. *P < 0.05, **P < 0.01 between groups; ns = non-significant.

6. **Figure 6. Terminal hepatic tissue transcript and protein analysis prior to the PM clamp.** (A) Experimental timeline for hepatic biopsies collected at 0 minutes (Basal) and 330 minutes (terminal, immediately before the PM clamp for each experimental group). Levels of Akt protein (B), glucokinase mRNA (C), glucokinase protein (D), intact microsome glucose-6-phosphatase activity using G6P and M6P substrates (E), glycogen synthase protein (F), glycogen phosphorylase protein (G), and glycogen phosphorylase activity (H) are shown. Data are presented for the Basal (n = 5), AM INS (n = 4), and AM INS+GCG (n = 4) groups as mean ± SEM. *P < 0.05, **P < 0.01 between groups; ns = non-significant. Protein levels were measured by western blot and mRNA levels by real-time qPCR. Protein levels were normalized to Ponceau S total protein; mRNA levels were normalized to GAPDH.

7. **Figure 7. Terminal hepatic tissue transcript and protein analysis after the PM clamp.** (A) Experimental timeline for hepatic biopsies collected at 0 minutes (Basal) and 480 minutes (terminal, end of the PM clamp for each experimental group). Levels of Akt protein (B), glucokinase mRNA (C), glucokinase protein (D), intact microsome glucose-6-phosphatase activity using G6P and M6P substrates for a subset of animals (n = 4/group; Basal not included; E), glycogen synthase protein (F), glycogen synthase activity (active/total; G), glycogen phosphorylase protein (H), glycogen phosphorylase activity (I), and mean direct glycogen synthesis during the PM clamp (J) are shown. Data are presented for the Basal

(n = 5), AM INS (n = 8), and AM INS+GCG (n = 8) groups as mean ± SEM. *P < 0.05, **P < 0.01, ***P < 0.001, ****P < 0.0001 between groups; ns = non-significant. Protein levels were measured by western blot and mRNA levels by real-time qPCR. Protein levels were normalized to Ponceau S total protein; mRNA levels were normalized to GAPDH.

8. **Figure 8. Summary of hepatic fluxes during the PM HIHG clamp.** The left panel shows the AM INS group (n = 8) and the right panel shows the AM INS+GCG group (n = 8). Values represent mean fluxes ± SEM from 360-480 min of the PM clamp, determined by carbon balance analysis. Depicted fluxes include glucose to/from glucose-6-phosphate (G6P), G6P to/from glycogen, and G6P to/from pyruvate through gluconeogenesis and glycolysis (estimated using alanine, glycerol, and lactate as 3-carbon precursors). The magnitude of the arrows reflects the relative flow in each pathway. Abbreviations: NHGU, net hepatic glucose uptake; HGU, hepatic glucose uptake; HGP, hepatic glucose production; Net HGU, net hepatic glucose uptake (HGU and HGP).

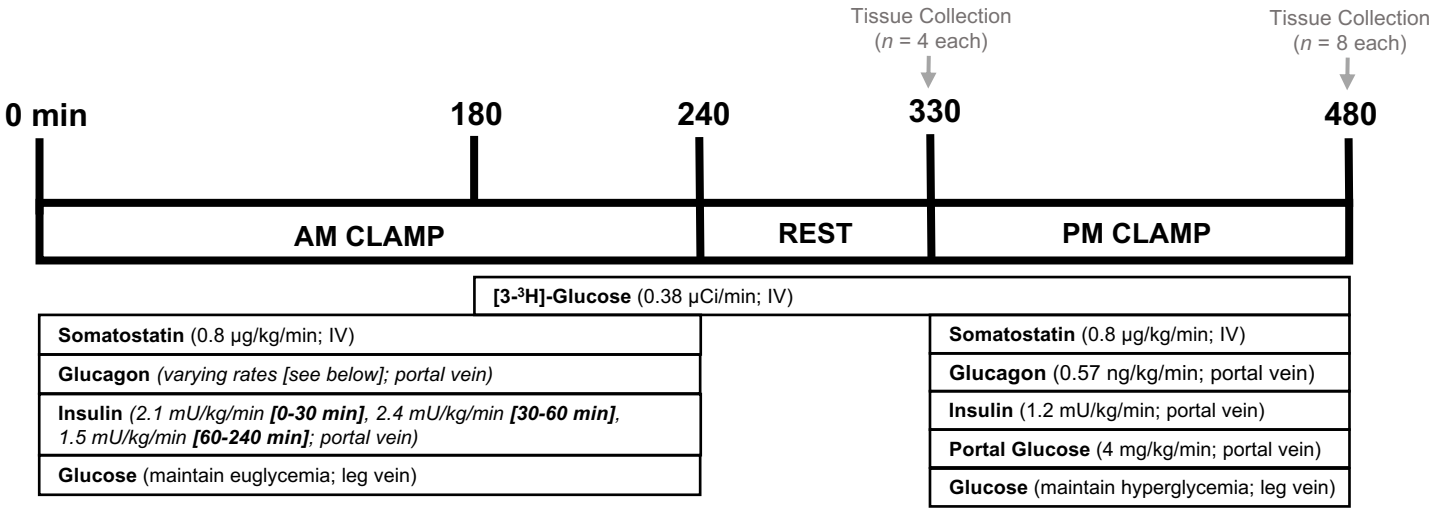

AM CLAMP GLUCAGON RATES (ng/kg/min):

AM INS (Basal glucagon, *n=8*):
0-240 min: 0.57

AM INS + GCG (Hyperglucagonemia, *n=8*):
0-30 min: 2.28
30-60 min: 2.60
60-240 min: 1.63

Figure 1. Experimental protocol. Canines underwent a 4h euglycemic clamp in the morning (AM; 0-240 min). Somatostatin (SST) was infused to suppress endogenous secretion of glucagon (GCG) and insulin (INS). Insulin was replaced in a pattern mimicking levels previously observed during a duodenal glucose infusion. One group received basal glucagon (AM INS), while the other received hyperglucagonemia (AM INS+GCG) in a pattern maintaining an equal molar ratio between insulin and glucagon throughout the AM clamp. A tracer infusion was initiated near the end of the AM clamp (180 min) to allow equilibration before the start of the PM clamp. Following the AM clamp, there was a 1.5h rest period (240-330 min) during which all infusions were halted. At the end of this period, a subset of dogs (*n* = *4*/group) was euthanized for hepatic tissue collection and molecular analysis. The remaining dogs (*n* = *8*/group) underwent a 2.5h PM hyperinsulinemic-hyperglycemic clamp with portal glucose delivery (330-480 min), after which hepatic tissue was collected. Additional details are provided in the Methods section.

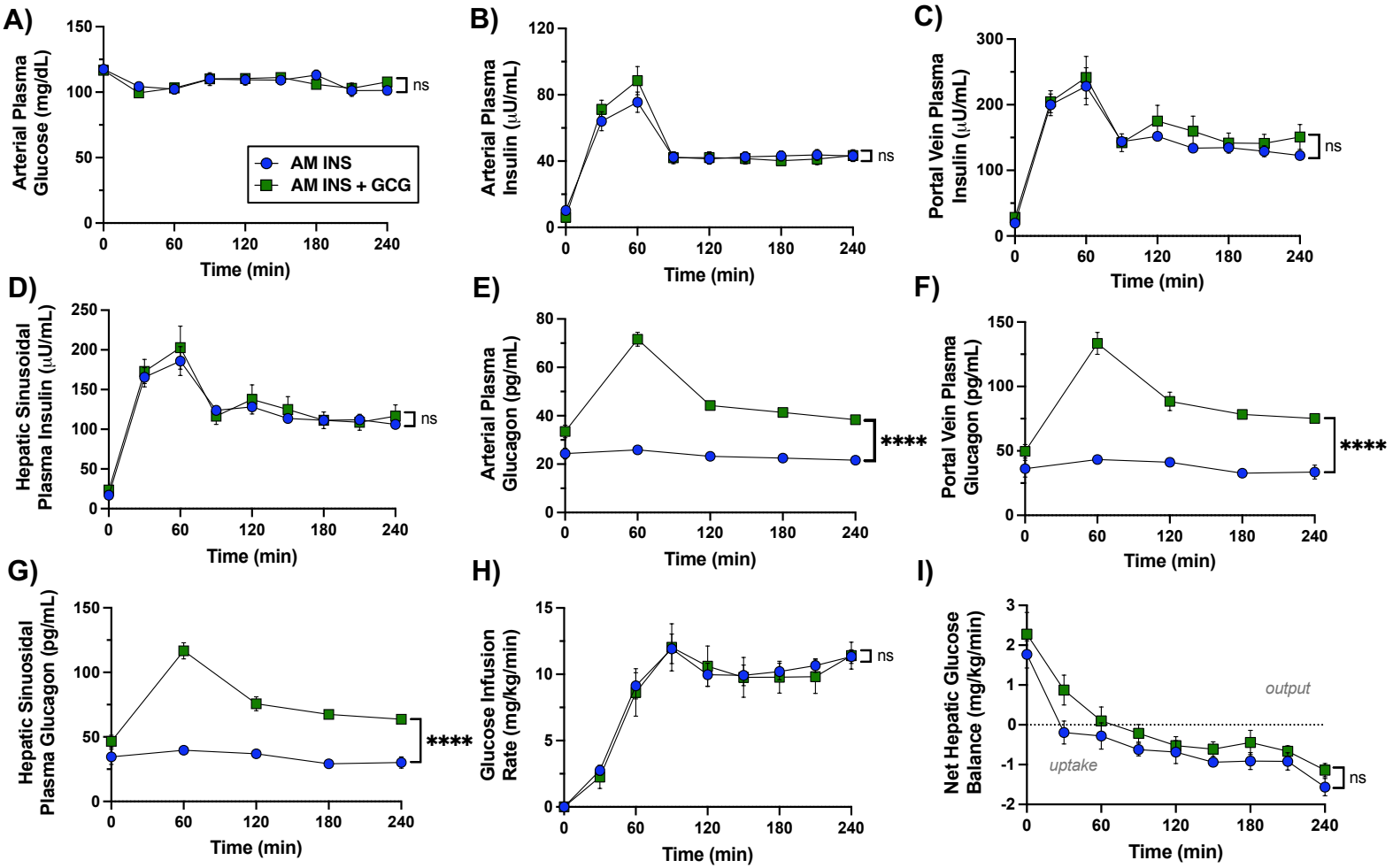

Figure 2. Morning (AM) clamp glucose and hormone flux data. (A) Arterial plasma glucose, (B) arterial plasma insulin, (C) portal vein plasma insulin, (D) hepatic sinusoidal plasma insulin, (E) arterial plasma glucagon, (F) portal vein plasma glucagon, (G) hepatic sinusoidal plasma glucagon, (H) glucose infusion rate, and (I) net hepatic glucose balance (negative values indicate uptake, positive values indicate output) are shown for the AM INS and AM INS+GCG groups (*n* = *8*/group) throughout the AM clamp. Data are expressed as mean ± SEM. ***P < 0.001, ****P < 0.0001 between groups; ns = non-significant.

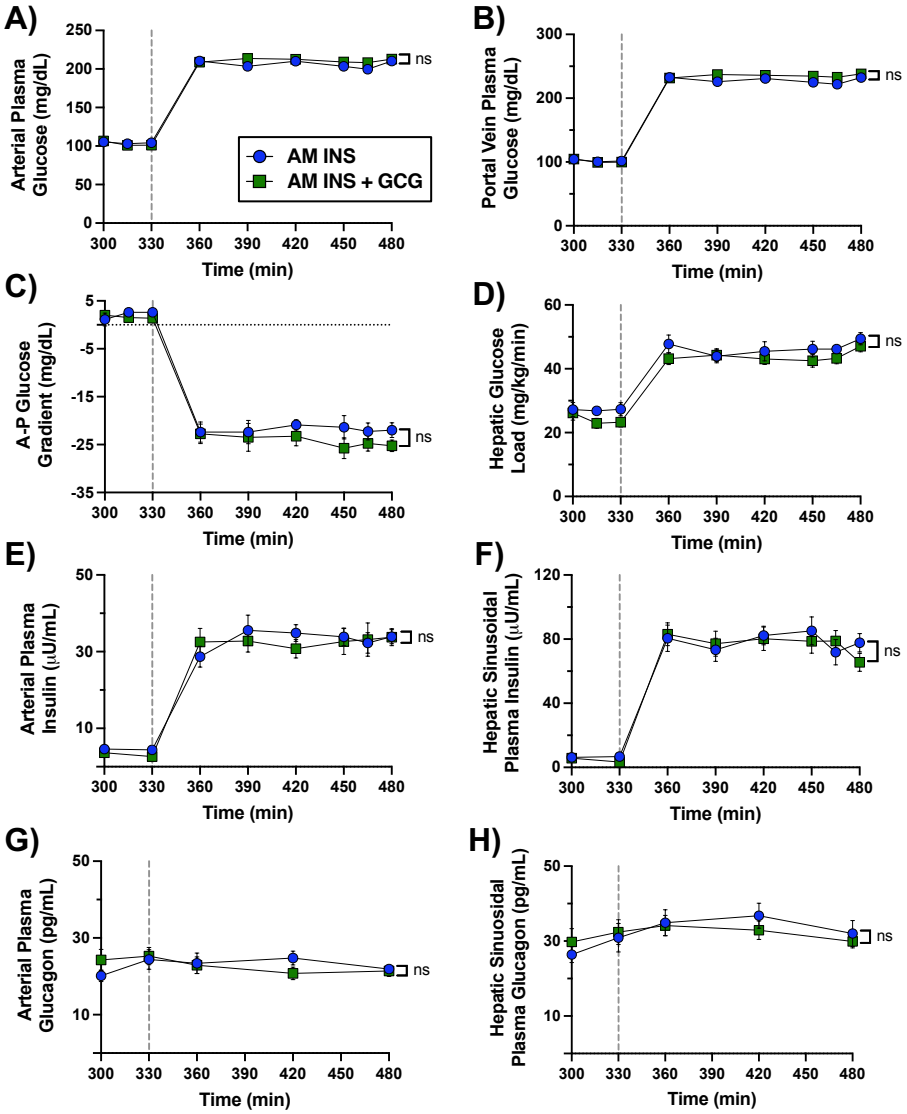

Figure 3. Afternoon (PM) clamp glucose and hormone flux data. A vertical line at 330 min indicates the end of the rest period and the onset of the PM clamp. (A) Arterial plasma glucose, (B) portal vein plasma glucose, (C) arterial–portal glucose difference, (D) hepatic glucose load, (E) arterial plasma insulin, (F) hepatic sinusoidal plasma insulin, (G) arterial plasma glucagon, and (H) hepatic sinusoidal plasma glucagon are shown throughout the 2.5h hyperinsulinemic-hyperglycemic PM clamp in both the AM INS and AM INS+GCG groups (*n* = *8*/group). No significant differences were observed between groups for any measured parameter. Data are expressed as mean ± SEM; ns = non-significant.

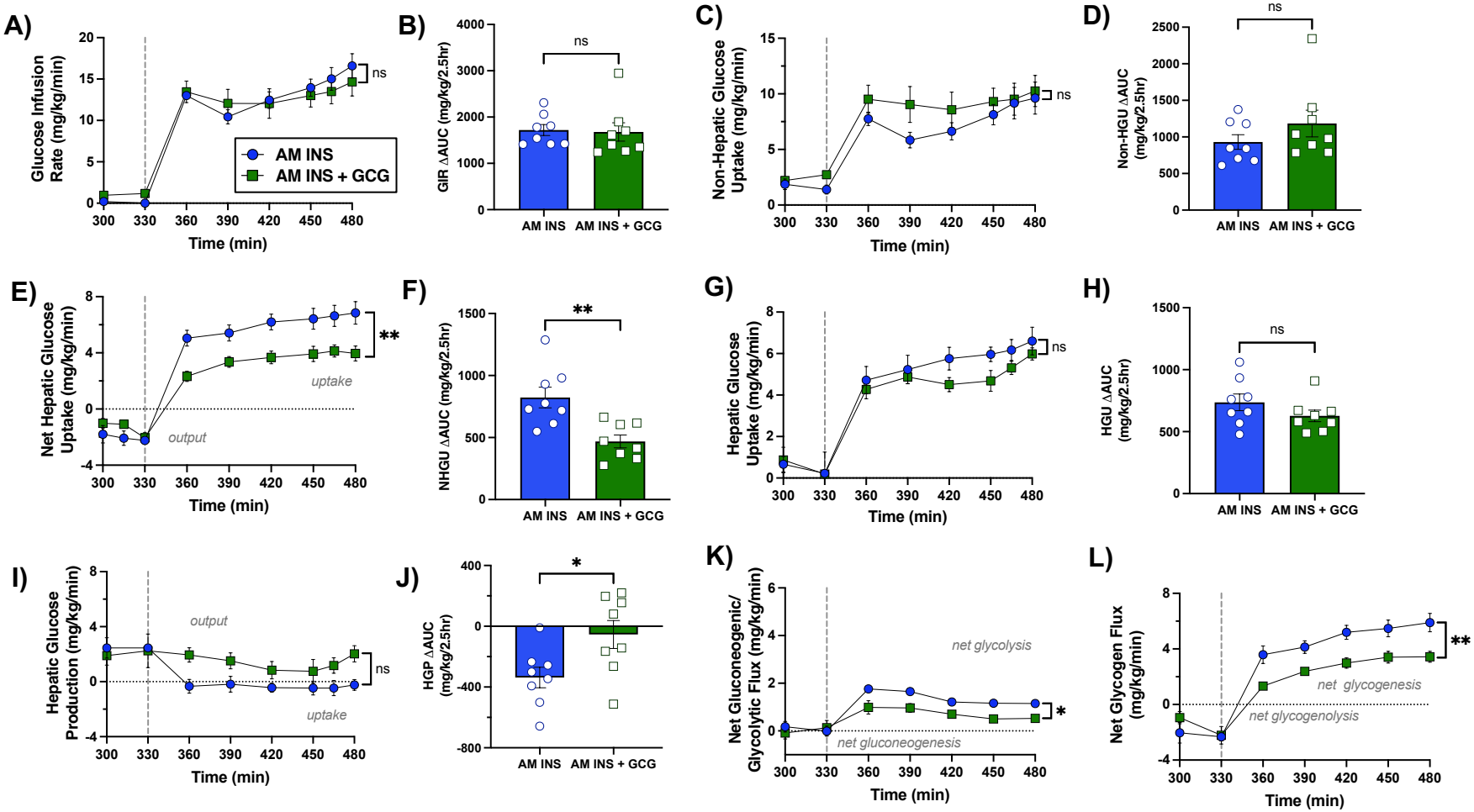

Figure 4. Glucose uptake and storage during the PM hyperinsulinemic-hyperglycemic clamp. A vertical line at 330 min indicates the end of the rest period and the onset of the PM clamp. (A) Glucose infusion rate (GIR), (B) GIR ΔAUC, (C) non-hepatic glucose uptake (NHGU), (D) NHGU ΔAUC, (E) net hepatic glucose uptake (NHGU; values >0 indicate uptake, <0 indicate output), (F) NHGU ΔAUC, (G) unidirectional hepatic glucose uptake determined using tritiated glucose, (H) HGU AUC, (I) hepatic glucose production (HGP; determined from the difference between NHGU and HGU), (J) HGP AUC, (K) net gluconeogenic/glycolytic flux (values >0 indicate net glycolysis, <0 indicate net gluconeogenesis), and (L) net glycogen flux (values >0 indicate net glycogenesis, <0 indicate net glycogenolysis) are shown over time for the AM INS and AM INS+GCG groups (n = 8/group). Data are expressed as mean ± SEM. *P < 0.05, **P < 0.01 between groups; ns = non-significant.

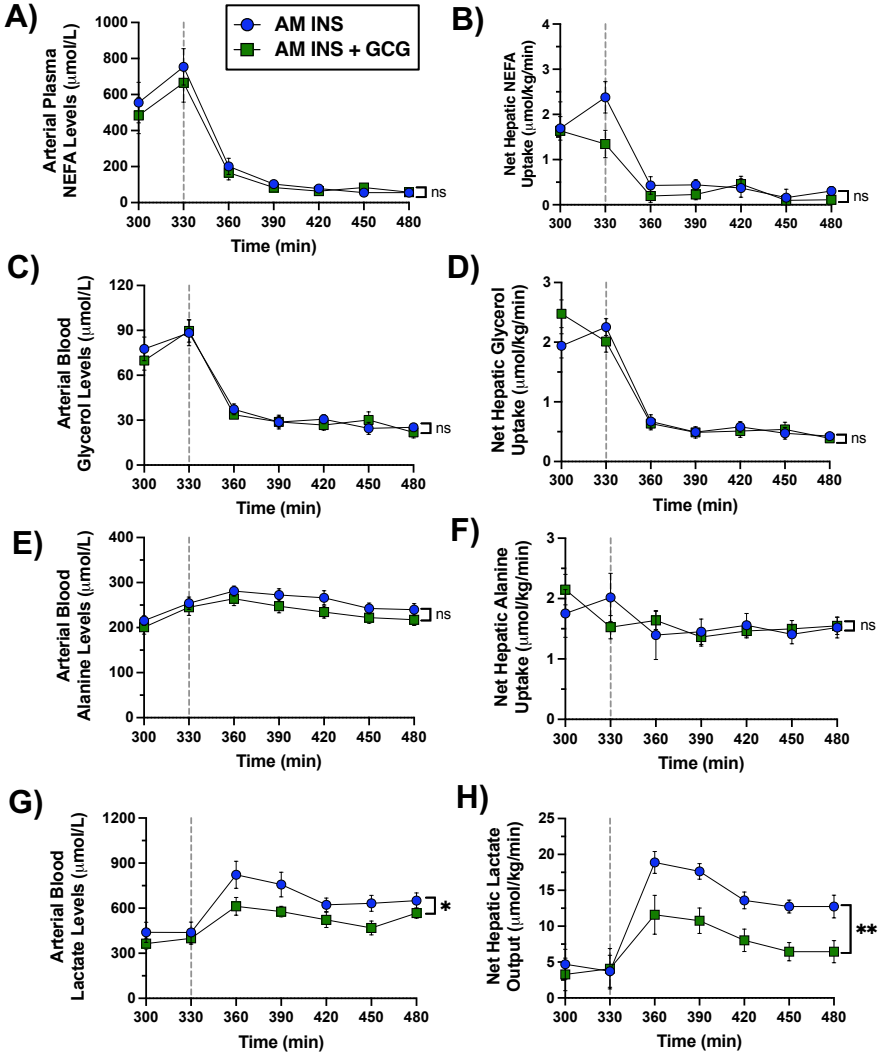

Figure 5: PM clamp fatty acid and metabolite flux data. A vertical line at 330 min separates the resting period from the onset of the PM clamp. (A) Arterial plasma non-esterified fatty acids (NEFA), (B) net hepatic NEFA uptake, (C) arterial blood glycerol, (D) net hepatic glycerol uptake, (E) arterial blood alanine, (F) net hepatic alanine uptake, (G) arterial blood lactate, and (H) net hepatic lactate uptake are shown throughout the PM HIHG clamp for the AM INS and AM INS+GCG groups ($n = 8$/group). Data are expressed as mean ± SEM. *P < 0.05, **P < 0.01 between groups; ns = non-significant.

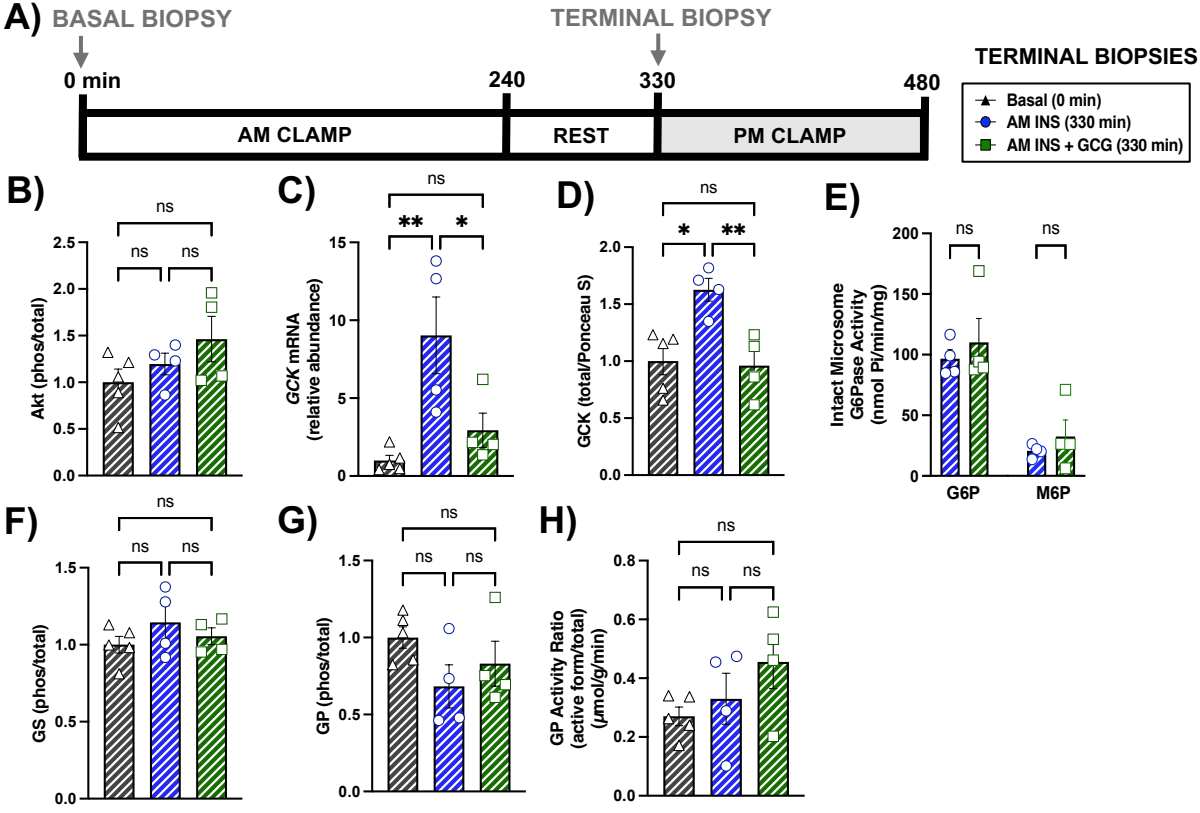

Figure 6. Terminal hepatic tissue transcript and protein analysis prior to the PM clamp.
(A) Experimental timeline for hepatic biopsies collected at 0 minutes (Basal) and 330 minutes (Terminal, immediately before the PM clamp). Levels of Akt protein (B), glucokinase mRNA (C), glucokinase protein (D), intact microsome glucose-6-phosphatase activity using G6P and M6P substrates (E), glycogen synthase protein (F), glycogen phosphorylase protein (G), and glycogen phosphorylase activity (H) are shown. Data are presented for the Basal (n = 5), AM INS (n = 4), and AM INS+GCG (n = 4) groups as mean ± SEM. Protein levels were normalized to Ponceau S total protein; mRNA levels were normalized to GAPDH. Statistical significance: *P < 0.05, **P < 0.01; ns = not significant. Protein levels were measured by western blot, mRNA levels by real-time qPCR, and enzyme activities by microsomal assays.

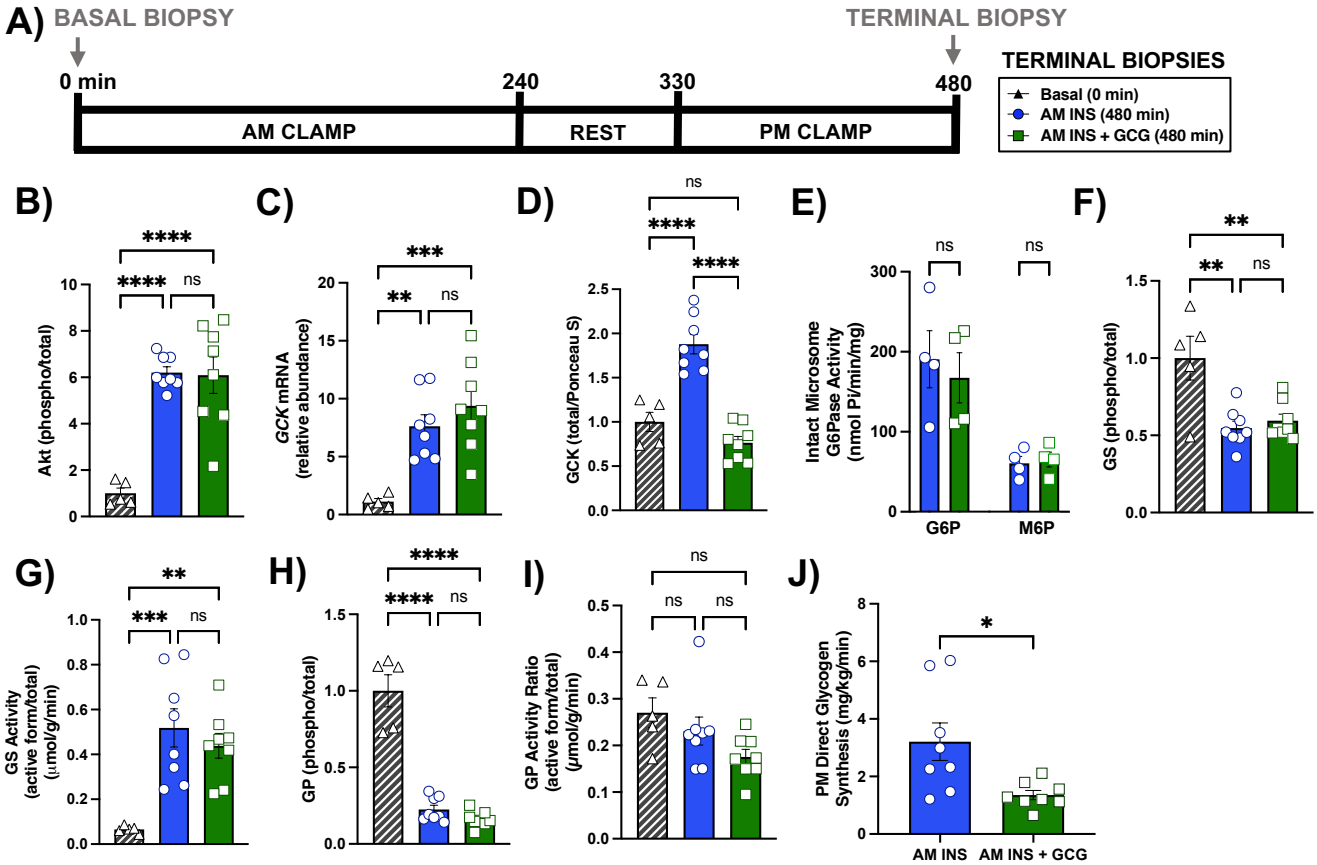

Figure 7. Terminal hepatic tissue transcript and protein analysis after the PM clamp. (A) Experimental timeline for hepatic biopsies collected at 0 minutes (Basal) and 480 minutes (terminal, end of the PM clamp for each experimental group). Levels of Akt protein (B), glucokinase mRNA (C), glucokinase protein (D), intact microsome glucose-6-phosphatase activity using G6P and M6P substrates for a subset of animals (n = 4/group; Basal not included; E), glycogen synthase protein (F), glycogen synthase activity (active/total; G), glycogen phosphorylase protein (H), glycogen phosphorylase activity (I), and mean direct glycogen synthesis during the PM clamp (J) are shown. Data are presented for the Basal (n = 5), AM INS (n = 8), and AM INS+GCG (n = 8) groups as mean ± SEM. *P < 0.05, **P < 0.01, ***P < 0.001, ****P < 0.0001 between groups; ns = non-significant. Protein levels were measured by western blot and mRNA levels by real-time qPCR. Protein levels were normalized to Ponceau S total protein; mRNA levels were normalized to GAPDH.

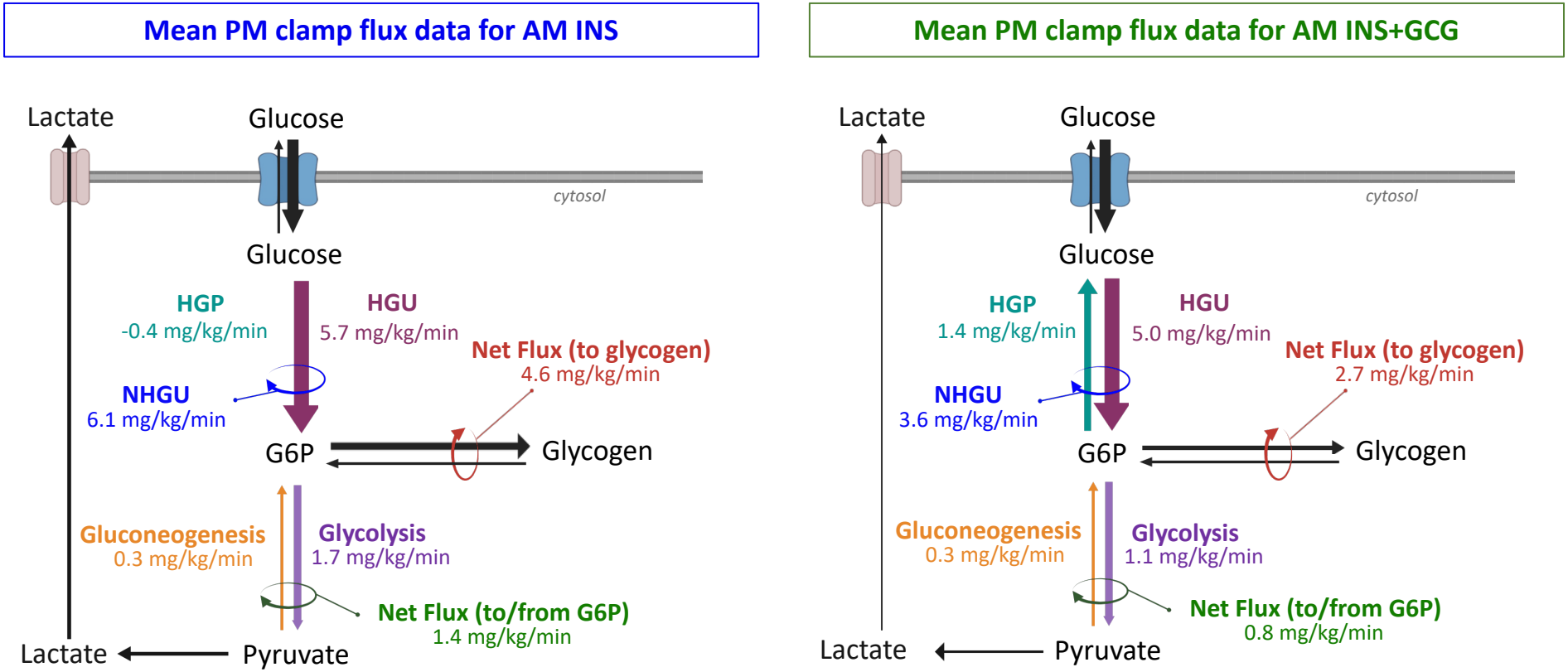

Figure 8. Summary of hepatic fluxes during the PM HIHG clamp. The left panel shows the AM INS group (*n* = *8*) and the right panel shows the AM INS+GCG group (*n* = *8*). Values represent mean fluxes ± SEM from 360-480 min of the PM clamp, determined by carbon balance analysis. Depicted fluxes include glucose to/from glucose-6-phosphate (G6P), G6P to/from glycogen, and G6P to/from pyruvate through gluconeogenesis and glycolysis (estimated using alanine, glycerol, and lactate as 3-carbon precursors). The magnitude of the arrows reflects the relative flow in each pathway. Abbreviations: NHGU, net hepatic glucose uptake; HGU, hepatic glucose uptake; HGP, hepatic glucose production; Net HGU, net hepatic glucose uptake (HGU and HGP).